

# Glassy nature of stripe ordering in $\text{La}_{1.6-x}\text{Nd}_{0.4}\text{Sr}_x\text{CuO}_4$

J. M. Tranquada

*Physics Department, Brookhaven National Laboratory, Upton, NY 11973-5000*

N. Ichikawa and S. Uchida

*Department of Applied Physics, The University of Tokyo, Yayoi 2-11-16, Bunkyo-ku,  
Tokyo 113, Japan*

(October 16, 1998)

We present the results of neutron-scattering studies on various aspects of crystalline and magnetic structure in single crystals of  $\text{La}_{1.6-x}\text{Nd}_{0.4}\text{Sr}_x\text{CuO}_4$  with  $x = 0.12$  and  $0.15$ . In particular, we have reexamined the degree of stripe order in an  $x = 0.12$  sample. Measurements of the width for an elastic magnetic peak show that it saturates at a finite value below 30 K, corresponding to a spin-spin correlation length of 200 Å. A model calculation indicates that the differing widths of magnetic and (previously reported) charge-order peaks, together with the lack of commensurability, can be consistently explained by disorder in the stripe spacing. Above 30 K (i.e., above the point at which a recent muon spin-rotation study has found a loss of static magnetic order), the width of the nominally elastic signal begins to increase. Interpreting the signal as critical scattering from slowly fluctuating spins, the temperature dependence of the width is consistent with renormalized classical behavior of a 2-dimensional anisotropic Heisenberg antiferromagnet. Inelastic scattering measurements show that incommensurate spin excitations survive at and above 50 K, where the elastic signal is negligible. Given that the stripe order is believed to be pinned by the low-temperature tetragonal (LTT) crystal structure, we have also investigated the transition near 70 K from the low-temperature orthorhombic (LTO) structure. We show that our  $x = 0.12$  crystal passes through an intervening less-orthorhombic phase, before reaching the LTT at  $\sim 40$  K, whereas the  $x = 0.15$  crystal goes directly from LTO to LTT, with coexistence of the two phases over a range of  $\sim 7$  K. Sharp Bragg peaks in the LTT phase of the  $x = 0.15$  crystal indicate a domain size of  $\gtrsim 1000$  Å, with no obvious evidence for LTO domains; hence, the coexistence of stripe order and superconductivity in this sample cannot be explained by a mixture of crystalline phases. Finally, we present scattering evidence for small LTT-like domains in the LTO phase of the  $x = 0.15$  sample. A correlation between the volume fraction of such domains and deviations of in-plane resistivity from linear  $T$  dependence suggest that charge stripes interact with these domains within the LTO matrix.

75.50.Ee, 75.30.Fv, 71.45.Lr, 71.27+a

## I. INTRODUCTION

Important insights into the spatial correlations of charge and spin in cuprate superconductors have been provided by studies of the  $x = \frac{1}{8}$  anomaly originally discovered<sup>1</sup> in  $\text{La}_{2-x}\text{Ba}_x\text{CuO}_4$ . Early on it was demonstrated by X-ray diffraction experiments that the anomalous suppression of superconductivity near  $x = \frac{1}{8}$  is associated with a modification of the crystal structure from the usual low-temperature orthorhombic (LTO) phase to the low-temperature tetragonal (LTT) variant.<sup>2,3</sup> After it was found that the same structural modification can be induced in  $\text{La}_{2-x}\text{Sr}_x\text{CuO}_4$  by partial substitution of Nd for La,<sup>4</sup> intensive efforts were focused on the latter system. A systematic study of the phase diagram revealed that not only the symmetry of the lattice modulation but also its amplitude is correlated with suppression of superconductivity and the appearance of local, static magnetism.<sup>5</sup> The discovery by neutron diffraction<sup>6,7</sup> of elastic superlattice peaks corresponding

to two-dimensional charge and spin order in a sample of  $\text{La}_{1.48}\text{Nd}_{0.4}\text{Sr}_{0.12}\text{CuO}_4$  suggested a likely explanation for the anomaly: the dopant-induced charge carriers, whose density is spatially modulated in a periodic fashion similar to an array of stripes, can be pinned by the lattice modulation in the LTT phase, with the pinning being strongest when the periodicity is commensurate, near  $x = \frac{1}{8}$ . With the charge stripes localized, the Cu moments in intervening regions can order antiferromagnetically, but with neighboring domains having an antiphase relationship induced by the charge. The suppression of superconductivity by the stripe pinning is compatible with at least one theoretical model for the cuprates,<sup>8</sup> in which the development of superconducting phase coherence is limited by the ability of hole pairs to tunnel between stripes. The Josephson coupling between stripes should be depressed by pinning.

There is a clear connection between the static correlations found in  $\text{La}_{1.6-x}\text{Nd}_{0.4}\text{Sr}_x\text{CuO}_4$  and the dynamic ones observed in good superconductors. For example, the

magnetic fluctuations in superconducting  $\text{La}_{2-x}\text{Sr}_x\text{CuO}_4$  are characterized by a doping-dependent incommensurate wave vector,<sup>9</sup> and, for a given Sr concentration, the wave vectors found in samples with and without Nd are essentially identical.<sup>10,11</sup> Also, elastic incommensurate magnetic peaks have now been observed in other superconducting systems, such as  $\text{La}_{2-x}\text{Sr}_x\text{Cu}_{1-y}\text{Zn}_y\text{O}_4$  (Ref. 12, 13, 14) and  $\text{La}_2\text{CuO}_{4+\delta}$  (Ref. 15). Furthermore, it has recently been shown that the magnetic fluctuations in underdoped  $\text{YBa}_2\text{Cu}_3\text{O}_{6+x}$  have an incommensurate component,<sup>16,17</sup> and that the spatial orientation of the modulation wave vector is identical with that in  $\text{La}_{2-x}\text{Sr}_x\text{CuO}_4$ . Thus, it may be possible to gain a better understanding of the dynamic correlations in the good superconductors by studying the static correlations in the Nd-doped system with depressed superconductivity.

A number of intriguing features have already been observed in the stripe-ordered phases. Contrary to observations on Fermi-surface-driven charge-density-wave (CDW) ordered systems,<sup>18</sup> infrared reflectivity studies indicate that there is no significant gap in the optical conductivity within the  $\text{CuO}_2$  planes.<sup>19</sup> Also, there is increasing evidence that bulk superconductivity and static stripe order can coexist.<sup>11,20,21,22</sup> Given these surprising results, it is important to investigate further the nature of the static stripe correlations. What is the nature of the order, both of the spins and of the underlying lattice modulation?

We have previously shown that the spin and charge order in  $\text{La}_{1.6-x}\text{Nd}_{0.4}\text{Sr}_x\text{CuO}_4$  with  $x = 0.12$  is quasi-two-dimensional.<sup>7,23</sup> Here we show that the ordering is somewhat glassy. Using high  $Q$  resolution measurements of an elastic magnetic peak, we find that the peak width  $\kappa$  saturates below  $\sim 30$  K, at a value corresponding to a spin-spin correlation length ( $= 1/\kappa$ ) of  $\sim 200$  Å. A model calculation, presented in the discussion section, demonstrates that the differing spin and charge-order peak widths<sup>23</sup>, together with the deviation from commensurability, are consistent with disorder in the charge-stripe spacing. The cause of the disorder is undetermined, but might be due to interactions between the holes and the  $\text{Sr}^{2+}$  dopant potentials.

A recent muon-spin-rotation ( $\mu\text{SR}$ ) study<sup>22</sup> indicates that, for  $x = 0.12$ , the static magnetic correlations disappear at approximately 30 K. In contrast, the nominally elastic magnetic peak detected with neutrons does not disappear until  $\sim 50$  K; however, we find that the peak width begins to grow for  $T \gtrsim 30$  K. The  $\mu\text{SR}$  result implies that the higher temperature neutron signal involves an integration over low frequency spin fluctuations. Under the assumption that the finite energy resolution integrates over the dominant critical fluctuations,  $\kappa$  corresponds to the inverse of the instantaneous spin-spin correlation length. The temperature dependence of  $\kappa$  is consistent with the renormalized-classical regime of an anisotropic Heisenberg antiferromagnet.<sup>24,25</sup> A fit to the data yields an estimate of the anisotropy of the effective magnetic exchange; however, in order to obtain consis-

tency with the narrow  $Q$ -width observed for spin fluctuations at  $\hbar\omega = 3$  meV, it is necessary to consider quantum effects such as those predicted when the magnetic domains correspond to even-legged spin ladders.<sup>26,27</sup>

We have also made a detailed study of the LTO to LTT transition in crystals with  $x = 0.12$  and 0.15. One significant result is that, for the  $x = 0.15$  sample, the LTT phase exhibits sharp Bragg peaks, with no obvious evidence for LTO domains. It follows that the stripe order and superconductivity observed<sup>11,20,22</sup> in this sample must come from the same crystallographic phase. In contrast, we do observed diffuse scattering consistent with LTT-like domains within the LTO phase for  $T \gtrsim 80$  K. The volume fraction of such domains is correlated with a deviation of the in-plane resistivity from linear  $T$  dependence. This correlation suggests that charge stripes may interact with the LTT-like domains, thus affecting the resistivity.

The rest of the paper is organized as follows. After a brief description of experimental details in the next section, characterizations of the LTO-to-LTT structural transition are presented in section III. In section IV, the high  $Q$  resolution study of elastic magnetic scattering for  $x = 0.12$  is reported. Some inelastic magnetic scattering measurements for the  $x=0.12$  and 0.15 compositions are presented in section V. In section VI, elastic diffuse scattering measurements near a forbidden superlattice position in the LTO phase of the  $x = 0.15$  sample are analyzed. Further discussion of the results, including the stripe-disorder model calculation, is presented in section VII.

## II. EXPERIMENTAL DETAILS AND NOTATION

The crystals of  $\text{La}_{1.6-x}\text{Nd}_{0.4}\text{Sr}_x\text{CuO}_4$  used in this work were grown at the University of Tokyo by the traveling-solvent floating-zone method. All are cylindrical rods 4 mm in diameter, with varying lengths. The elastic scattering studies of the  $x = 0.12$  composition were performed on crystal U2, which is approximately 10 mm in length. The corresponding inelastic measurements were done on crystal U3, which was originally 40 mm in length, but which eventually fell into pieces due to hydration of small, poorly reacted inclusions. Pieces of the latter crystal were used in the X-ray diffraction study of charge-order scattering reported in Ref. 23. For the  $x = 0.15$  composition, crystal U6 (35 mm in length) was used. An earlier crystal of the same composition (U4) was used for the measurements reported in Ref. 11. That crystal suffered the same fate as U3, and a piece of it was later used for the magnetization study described in Ref. 20.

The neutron-scattering studies were performed on triple-axis spectrometers H4M and H7 at the High Flux Beam Reactor, located at Brookhaven National Laboratory. Pyrolytic graphite (PG) monochromators and analyzers were used, and the (002) reflection was em-

ployed in all cases, except for certain elastic, high  $Q$ -resolution measurements of strong Bragg peaks, where the analyzer was set to the (004) reflection. Essentially all measurements were done with an incident neutron energy of 14.7 meV, with one or more PG filters in the incident beam to minimize the neutron flux at higher-harmonic wavelengths. Each crystal was cooled in a Displex closed-cycle He refrigerator, with the temperature monitored by a Si diode.

As mentioned in the introduction, the three crystal structures of relevance to the present work are the LTO, LTLO, and LTT, which correspond to the  $Bmab$ ,  $Pccn$ , and  $P4_2/nm$  space groups, respectively.<sup>4,28</sup> All of these structures have a unit cell with lattice vectors  $\mathbf{a}$  and  $\mathbf{b}$  rotated by  $45^\circ$  with respect to the Cu-O bonds in the  $\text{CuO}_2$  planes. When we specify a reflection in reciprocal lattice units ( $2\pi/a_o, 2\pi/b_o, 2\pi/c$ ) with respect to this cell, we will denote it with a subscript  $o$  for “orthorhombic”. (In the LTT phase at 10 K,  $a_o = 5.34 \text{ \AA}$  and  $c = 13.1 \text{ \AA}$ .) To describe the magnetic scattering, it is more convenient to work with respect to a smaller cell with lattice vectors parallel to the in-plane Cu-O bonds. In this case, the reciprocal lattice units are  $(2\sqrt{2}\pi/a_o, 2\sqrt{2}\pi/b_o, 2\pi/c)$ , and no subscript will be appended to the reciprocal-space coordinates.

### III. LTO-TO-LTT TRANSITION

In order to interpret the nature of the magnetic order, it is first necessary to characterize the underlying crystalline order. As a starting point, Fig. 1 shows the difference between the in-plane lattice parameters,  $b - a$ , as a function of temperature for two samples. The  $x = 0.15$  crystal transforms directly from LTO to LTT, with a coexistence of significant fractions of the two phases between 71 and 77 K (see Fig. 3 below). In contrast, the  $x = 0.12$  sample shows a large but incomplete decrease in the orthorhombic splitting at approximately 69 K.

The measurements on the  $x = 0.12$  sample require a bit of explanation. In the LTO phase, there are four possible orientations of twin domains. With the large mosaic crystals commonly studied, one typically finds the simultaneous presence of all four domain orientations, with comparable populations of the four domains. As a result, a scan along the  $[100]_o$  direction through a Bragg peak at  $(H00)_o$  will also detect a twin-related peak corresponding to  $(0H0)_o$ . Such is the case for the  $x = 0.15$  sample, and it allows one to measure the orthorhombic splitting with a single scan. With the  $x = 0.12$  crystal (U2), on the other hand, a single domain dominates (and there are a total of 3, rather than 4, domains, with unusual relative orientations). As a result, it is necessary to separately scan the  $(H00)_o$  and  $(0H0)_o$  reflections. An advantage of this situation is that, because the peaks do not overlap, we can achieve a better resolution of small changes in orthorhombicity. On the other hand, our absolute measure

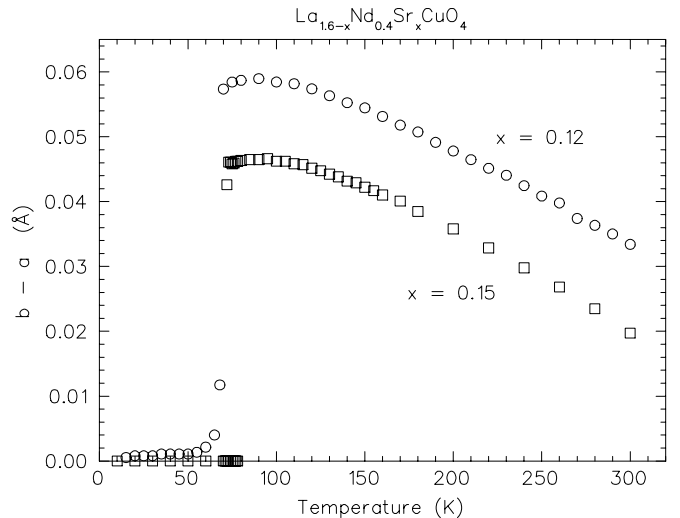


FIG. 1. Temperature dependence of the difference in in-plane lattice parameters,  $b - a$  (based on LTO unit cell), for the  $\text{La}_{1.6-x}\text{Nd}_{0.4}\text{Sr}_x\text{CuO}_4$  crystals with  $x = 0.12$  (circles) and  $x = 0.15$  (squares).

of orthorhombicity is limited by the precision with which the crystal is aligned.

The splitting measured for the  $x = 0.12$  crystal below the structural transition temperature is shown in Fig. 2. The error bar indicates twice the maximum variation in splitting between cooling and warming cycles (and corresponds to 4% of the peak width). The absolute uncertainty is certainly much greater than this, and we cannot establish from these measurements whether the crystal is tetragonal or orthorhombic at low temperature. It is certain that any remaining orthorhombicity below  $\sim 40$  K is extremely small, and, based on powder diffraction studies of samples with the same composition,<sup>4,5,29</sup> we expect that the crystal is actually tetragonal. The significant point is that the splitting grows monotonically between 50 K and the transition at 69 K. This behavior is consistent with the occurrence of an intervening LTLO phase, as first observed by Crawford *et al.*<sup>4</sup>. A corresponding feature is the increase in integrated intensity for the  $(200)_o$  and  $(020)_o$  Bragg peaks (see Fig. 2), which was seen previously in a single-crystal study by Shamoto *et al.*<sup>30</sup> The most likely explanation for the intensity variation is a reduction in extinction due to strain associated with the growing orthorhombicity. Assuming this to be the correct interpretation, the intensity provides a more precise measure of the structural changes, and it suggests that the crystal is essentially tetragonal, and no longer changing, for  $T \lesssim 40$  K.

Turning to the  $x = 0.15$  crystal, Fig. 3 shows high-resolution elastic scans through the  $(040)_o/(400)_o$  Bragg peaks. At 80 K, the LTO peaks are sharp and well separated; however, close inspection reveals a weak and broad contribution centered midway between the strong peaks. A similar feature has recently been observed in an X-ray powder diffraction study by Moodenbaugh *et al.*,<sup>29</sup> and

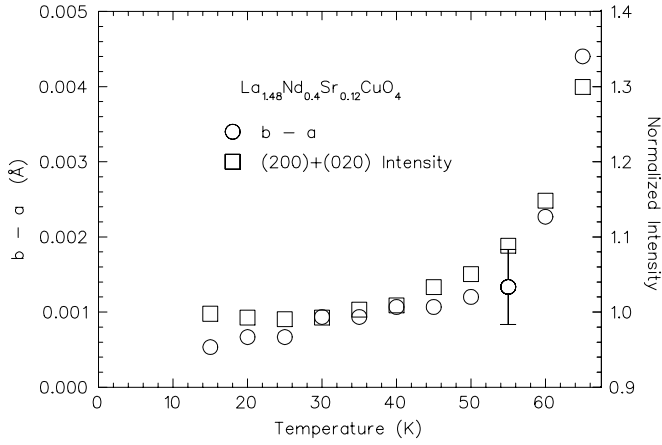


FIG. 2. Comparison between the orthorhombic splitting,  $b - a$ , (circles) and the average intensity of the (200) and (020) Bragg peaks (squares), normalized at low temperature.

interpreted as evidence for small LTT-like domains. We will return to that issue in section VI. For now, we focus on the sharp LTT peak that begins to appear below 78 K. As indicated in (b) and (c), there is coexistence of the LTO and LTT phases down to approximately 71 K. (Moodenbaugh *et al.*<sup>29</sup> observed a broader coexistence region of approximately 30 K in their powder study.) While a single, strong LTT peak dominates at 70 K, there is also a very weak component with a width roughly 3 times greater that lies under it.

The point to be emphasized here is the narrow width of the dominant LTT peak at 70 K. It is only marginally broader than the LTO peaks at 80 K, and all are close to the resolution width. Taking the resolution into account, we estimate a typical domain size of  $\sim 1000$  Å or greater. The LTT peak observed in this crystal is considerably sharper than those typically detected in powder samples,<sup>2,4,31</sup> where the LTT peak width is comparable to the LTO splitting. The broad peaks observed in powders raised concerns that the superconductivity which appears to survive in the LTT phase<sup>20,21,22</sup> might actually be associated with small LTO domains. In light of the present results, such a possibility seems quite unlikely.

#### IV. ELASTIC MAGNETIC SCATTERING

As discussed elsewhere,<sup>6,7</sup> magnetic superlattice peaks are observed within the  $(h, k, 0)$  zone of reciprocal space below approximately 50 K for  $x = 0.12$ , and 45 K for  $x = 0.15$ . Below  $\sim 3$  K, where the Nd moments start to order via coupling to the ordered Cu moments, thus enhancing the superlattice intensity with their much larger moments, it was possible to investigate the correlation lengths. Within the planes, the correlation length was found to be substantial but finite, while the magnetic correlations along the  $c$  axis are very short-range.<sup>7</sup> It was difficult to investigate the in-plane correlation length at

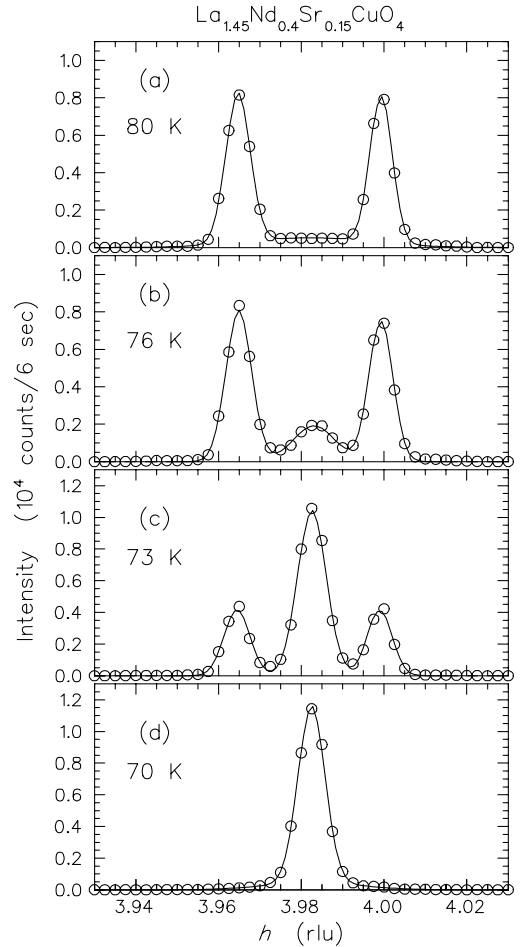


FIG. 3. Scans of the  $(040)_o/(400)_o$  Bragg peaks at several temperatures through the transition from the LTO phase (a), to the LTT phase (d), with coexistence of the two phases at intermediate temperatures, (b) and (c). Measured at H7 using  $E_i = 14.7$  meV, horizontal collimations =  $10'-10'-10'-10'$ , monochromator = PG(002), analyzer = PG(004).

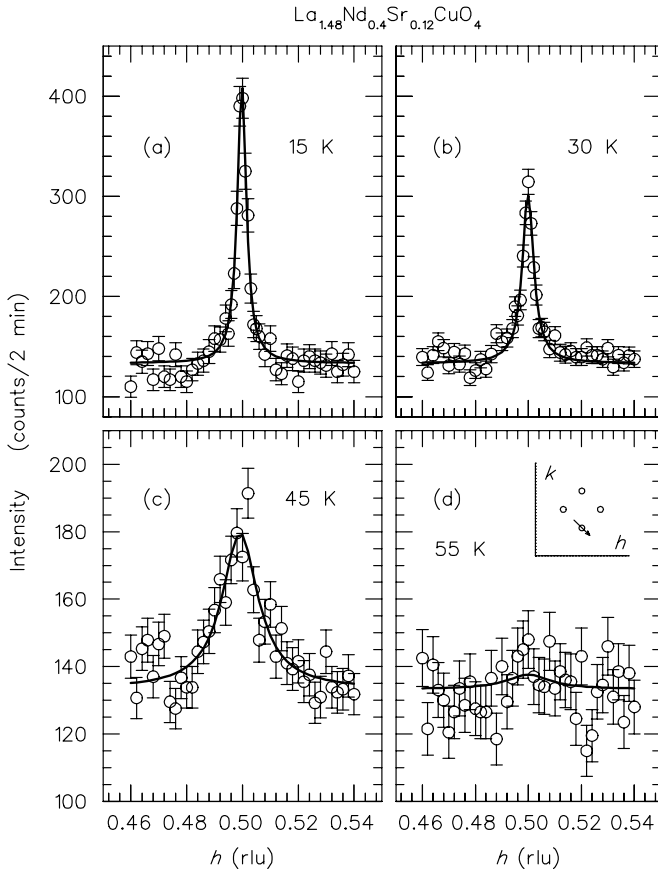


FIG. 4. Elastic scans in the transverse direction (see inset) through the magnetic superlattice peak at  $(0.5, 0.382)$  in  $\text{La}_{1.48}\text{Nd}_{0.4}\text{Sr}_{0.12}\text{CuO}_4$  for several different temperatures. The solid lines through the data points are fits to a Lorentzian plus constant background. Note the change in the intensity scale between (b) and (c). Measured at H4M using  $E_i = 14.7$  meV, horizontal collimations =  $40'-80'-20'-80'$ .

higher temperatures because the weakness of the intensity limited the degree to which it was practical to obtain sufficient  $Q$  resolution with tightened collimation.

Making another attempt, we have now succeeded in following the temperature dependence of the peak widths by performing transverse scans, where we can take advantage of the intrinsically tight resolution at small  $Q$ . Examples of such scans are presented in Fig. 4. The fitted peak shape corresponds to a Lorentzian plus constant background. (No systematic temperature dependence was found for the background, so the background value averaged over essentially all temperatures was applied and held fixed in the final fits.) An alternative peak shape has been suggested based on the recently proposed analogy between charge stripes and liquid crystals.<sup>32</sup> If the pinned stripes behave like a smectic liquid crystal, then one might expect the spatial correlations to decay algebraically, rather than exponentially.<sup>33</sup> In that case, the peak shape in reciprocal space would be proportional to  $(Q - Q_0)^{-p}$ . However, if the exponent  $p$  is close to 2,

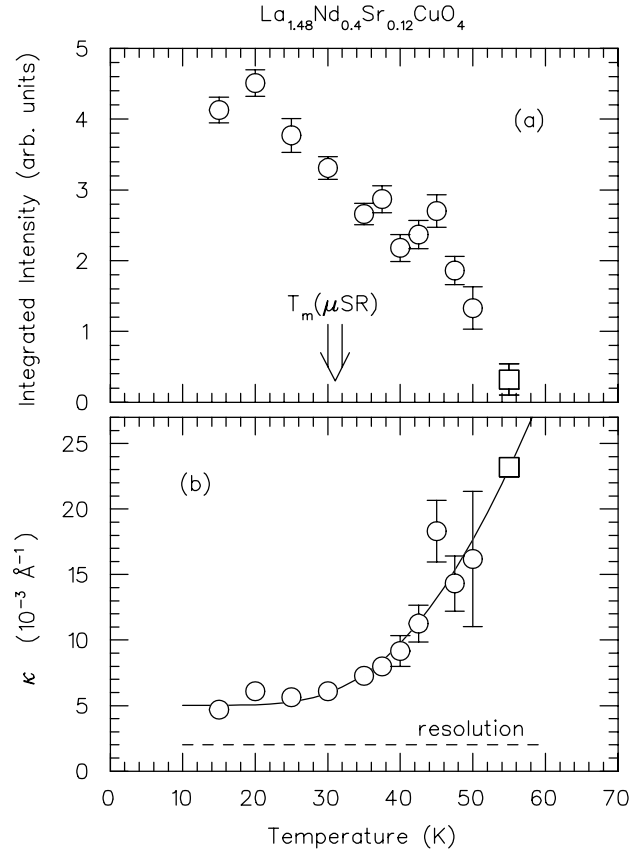


FIG. 5. Results of the Lorentzian fits to the magnetic peak scans, as a function of temperature. (a) Integrated intensity (in arbitrary units); arrow indicates the magnetic ordering temperature detected by  $\mu\text{SR}$  (Ref. 22). (b) Peak half-width,  $\kappa$ ; dashed line indicates resolution half-width; line through points is discussed in the text. In fitting the scan at  $T = 55$  K (squares), the width was constrained to lie on the curve, and only the amplitude was varied.

one would need a much better signal-to-noise ratio and excellent knowledge of the background in order to distinguish the algebraic line shape from a Lorentzian. Further experimental advances will be required to test for such differences.

Results for the integrated intensity and peak half-width at half-maximum,  $\kappa$ , are shown as a function of temperature in Fig. 5. As indicated in (b), the resolution width is much less than the measured width, thus justifying the absence of a resolution correction in the fitting. Considering first the intensity, it is interesting to compare with a recent muon-spin-rotation ( $\mu\text{SR}$ ) study of magnetic order in a similar crystal.<sup>22</sup> There, a loss of order was detected near 30 K, as indicated by the arrow in Fig. 5(a). In contrast, the “elastic” signal seen by neutron scattering appears to survive up to approximately 50 K. Such an apparent conflict has been found previously<sup>34,35</sup> in studies of magnetic correlations in  $\text{La}_{2-x}\text{Sr}_x\text{CuO}_4$  with  $x \sim 0.05$ . It can be understood in terms of the distinct sensitivities of the two techniques to

fluctuations. In  $\mu$ SR, the local hyperfine field is considered static when it does not vary significantly on the time scale of the muon lifetime,  $\sim 2 \mu\text{s}$ . On the other hand, the neutron measurement integrates over fluctuations within a Gaussian resolution window with a full width at half maximum of approximately 0.8 meV (0.2 THz). Thus, the observations indicate that between 30 K and 50 K there is no static order, but instead there is a characteristic fluctuation rate that is gradually increasing from  $10^6$  to  $10^{11}$  Hz.

The temperature dependence of  $\kappa$  is qualitatively consistent with the above scenario. Below 30 K,  $\kappa$  remains constant. Taking the inverse of  $\kappa$  at low temperature gives a correlation length of 200 Å. Above 30 K,  $\kappa$  starts to increase. The curve through the data points corresponds to a fit with the form

$$\kappa = \kappa_0 + Ae^{-B/k_B T}, \quad (1)$$

which is essentially the formula used by Keimer *et al.*<sup>35</sup> to describe the inverse correlation length in lightly doped  $\text{La}_2\text{CuO}_4$ . The fit yields the following parameter values:  $\kappa_0 = 0.0050(2) \text{ \AA}^{-1}$ ,  $A = 0.6(6) \text{ \AA}^{-1}$ , and  $B = 17(4) \text{ meV}$ , where the estimated uncertainty in the last digit is listed in parentheses.

The second term on the right-hand side of Eq. (1) has the form predicted for the 2D quantum antiferromagnetic Heisenberg model in the renormalized classical regime.<sup>36,37</sup> Fits to experimental measurements of  $\kappa(T)$  in pure and lightly-doped  $\text{La}_2\text{CuO}_4$  by Keimer *et al.*<sup>35</sup> yielded  $B \approx J$ , where  $J$  is the exchange energy between nearest-neighbor Cu spins. It is not immediately clear that such a formula, based on a spin-only model, should be relevant to the present case, where there is a substantial concentration of holes in the planes. Castro Neto and Hone<sup>24</sup> have argued that within the stripe model, where the holes are restricted to moving along antiferromagnetic domain walls, the main effect of the holes would be to weaken the effective exchange between spins on either side of a domain wall. Assuming that this weakened coupling is the dominant factor for determining long-wavelength excitations along the modulation direction, they obtain an effective anisotropic Heisenberg model. Analysis of  $\kappa(T)$  based on that model yields the same exponential dependence on the inverse temperature,<sup>24,25</sup> as obtained in the isotropic case, but with modifications to the relationship between  $B$  and  $J$ .

Let  $\alpha$  represent the value of the effective exchange perpendicular to the stripes relative to the exchange parallel to the stripes. Then, according to Ref. 24,

$$B = 2\pi\rho_s(\alpha), \quad (2)$$

with

$$\rho_s(\alpha) = \sqrt{\alpha}JS^2, \quad (3)$$

where  $S = \frac{1}{2}$  is the spin. If we assume  $J$  to have the same value as in  $\text{La}_2\text{CuO}_4$  ( $\approx 135 \text{ meV}$ <sup>38</sup>), then from the

fitted value of  $B$  we find  $\alpha \approx 0.01$ . Going further, the theoretical expression for  $A$  is<sup>24</sup>

$$A \approx 8\sqrt{2}\pi\alpha^{\frac{1}{4}}/ae, \quad (4)$$

where  $a$  is the lattice parameter. Plugging in  $\alpha \approx 0.01$  gives  $A \approx 0.5$ , in good agreement with the fitted value.

Within the anisotropic Heisenberg model,<sup>24,25</sup> the spin-wave velocity perpendicular to the stripes (along the modulation direction) is

$$c_{\perp} \approx \sqrt{\frac{\alpha}{2}}c_0, \quad (5)$$

where  $c_0$  is the spin-wave velocity of the undoped antiferromagnet. The fitted value of  $\alpha$ , together with the experimental<sup>39</sup>  $c_0$  for  $\text{La}_2\text{CuO}_4$ , gives  $\hbar c_{\perp} \approx 50 \text{ meV}\text{-\AA}$ . We can use this result to check the assumption that the neutron measurement is integrating over low-energy fluctuations for  $T \gtrsim 30 \text{ K}$ . Neutrons measure the dynamic susceptibility,  $\chi''(\mathbf{Q}, \omega)$ , multiplied by  $1/(1 - e^{-\hbar\omega/k_B T})$ . Integrating over  $\mathbf{Q}$ , there is a peak in this quantity at  $\Gamma \approx \hbar c_{\perp} \kappa$ . Using the numbers above, we find  $\Gamma \approx 0.2 \text{ meV}$  at 30 K, and  $\Gamma \approx 0.8 \text{ meV}$  at 50 K, where the signal is disappearing. The former value is smaller than the energy resolution half-width, while the latter is larger. Thus, our interpretation appears reasonable. On the other hand, we will show in the next section that  $\hbar c_{\perp} \approx 50 \text{ meV}\text{-\AA}$  is much too small to be compatible with the observed low-energy inelastic scattering. It is also incompatible with the range of energies over which incommensurability is observed<sup>40,41</sup> in  $\text{La}_{2-x}\text{Sr}_x\text{CuO}_4$  with  $x \approx 0.15$ .

One solution to this dilemma is suggested by the analysis of Tworzydło *et al.*<sup>26</sup> They have pointed out that when the magnetic domains become sufficiently narrow (small stripe spacing) one can view them as coupled spin ladders. For small  $\alpha$ , one obtains qualitative differences depending on whether the spin ladders have an even or odd number of legs. (This distinction is absent in the original treatment of the anisotropic Heisenberg model.<sup>24,25</sup>) In particular, Tworzydło *et al.*<sup>26</sup> have shown that for 2-leg ladders a quantum-disordered state occurs for  $\alpha \leq 0.30$ . (For 4-leg ladders,<sup>27</sup> the transition is at  $\alpha = 0.07$ .) In terms of the 2-leg ladder model, our observed temperature dependence of  $\kappa$  could be explained with  $\alpha \approx 0.35$ , which would also be consistent with relatively stiff spin waves.<sup>26</sup>

Tworzydło *et al.*<sup>26</sup> have suggested that the 2-leg ladder model could be appropriate at  $x = \frac{1}{8}$  if the hole stripes are centered on O rows<sup>42</sup> in a manner such that they tie up the spins on the immediately adjacent rows of Cu. If this were the case, then tuning  $x$  away from  $\frac{1}{8}$  should introduce odd-leg ladders, which would presumably enhance the tendency for magnetic order.<sup>27</sup> In contrast, experiments<sup>11,43,14</sup> indicate that the highest magnetic ordering temperature actually occurs at  $x \approx 0.12$ . Thus, while the spin-only models can explain several features of the measurements, questions still remain. It is

quite possible that the fluctuations of the charge stripes, which are ignored in spin-only models, play a significant role in determining the spin correlations.

One other puzzle concerns the saturation of  $\kappa$  below 30 K. If the characteristic energy for critical spin fluctuations were 0.2 meV (or perhaps higher), then most of the spin fluctuations would be too fast to allow any muon precession to be observable. One possibility is that our analysis is too simple minded. Alternatively, it may be that the lack of temperature dependence in  $\kappa$  at low  $T$  is associated with disorder in the charge-stripe array, rather than with the temperature dependence of the spin fluctuations. Analysis of such a disorder model is presented in section VII.

## V. INELASTIC MAGNETIC SCATTERING

It is also interesting to characterize the spin dynamics directly through measurements of inelastic scattering. Figure 6 shows results for  $x = 0.12$  obtained by scanning through the incommensurate positions, along  $Q = (h, 0.5, 0)$ , with the energy transfer fixed at 2 meV [(a),(b),(c)] and at 3 meV [(d),(e),(f)]. A linear background has been subtracted, corrections have been made for differences in resolution volume at the two energies, and the thermal factor has been divided out, so that the resulting signal is proportional to  $\chi''(\mathbf{Q}, \omega)$ . The scattering is peaked rather sharply about the incommensurate wave vectors defined by the elastic scans, with the  $Q$ -width limited by resolution at 50 K. The signal is relatively strong at 50 K, and gradually decreases as the temperature is raised. At 72 K, above the transition to the LTO phase, the signal is still finite at 3 meV. This last result provides an important connection with studies<sup>40,41</sup> of spin fluctuations in  $\text{La}_{2-x}\text{Sr}_x\text{CuO}_4$ , where the structure is LTO. The LTT phase induced by Nd substitution appears to stabilize a static component of correlations that already exist dynamically in the LTO phase.

Inelastic measurements have also been performed on an  $x = 0.15$  sample. Results for the local susceptibility,  $\tilde{\chi}''(\omega) = \int d\mathbf{Q}_{2D} \chi''(\mathbf{Q}, \omega)$ , at two excitation energies, 1.75 and 3.5 meV, are presented as a function of temperature in Fig. 7.  $\tilde{\chi}''(\omega)$  changes relatively little between 10 and 40 K, where an elastic magnetic signal is observed. Above the neutron-determined ordering temperature ( $\sim 45$  K), the signal at 1.75 meV falls off rapidly, whereas the susceptibility at 3.5 meV appears to decrease more slowly. This behavior is qualitatively similar to the decay of the low-energy spin-fluctuation intensity in  $\text{La}_2\text{CuO}_4$  above  $T_N$ .<sup>44</sup>

Finally, it is interesting to compare the  $Q$ -width of the excitations in the  $x = 0.12$  crystal with that found in  $\text{La}_{2-x}\text{Sr}_x\text{CuO}_4$  with  $x = 0.15$ . Figure 8 shows scans for two such samples obtained under similar conditions:  $\hbar\omega = 3$  meV and  $T = 40$  K. The curve through the data in (b) is a Gaussian plus a linear background, while the

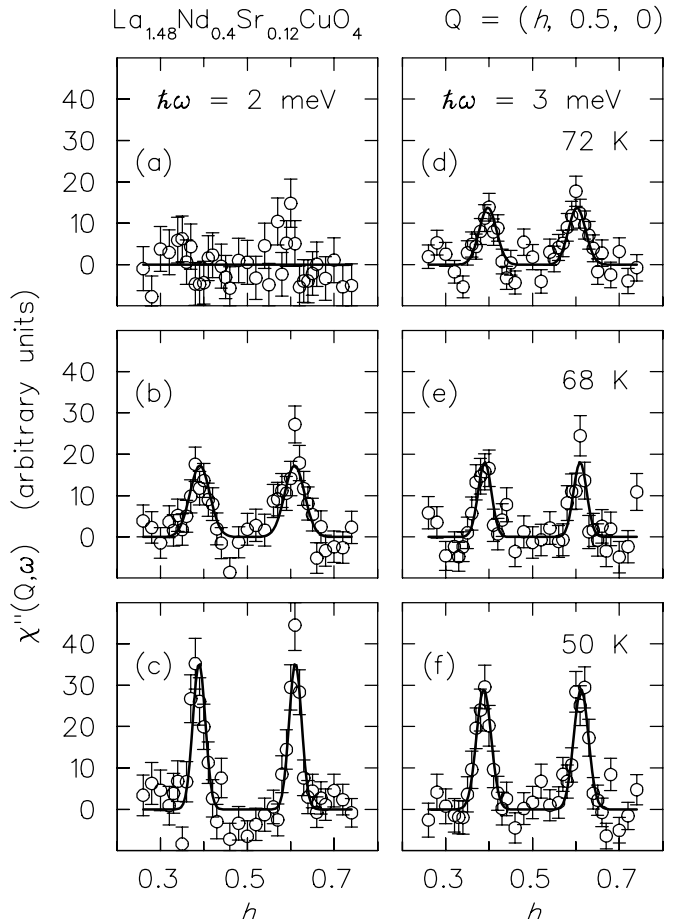


FIG. 6. Constant-energy scans along  $Q = (h, 0.5, 0)$ , through the magnetic wave vectors  $h = 0.5 \pm \epsilon$ , for  $\text{La}_{1.48}\text{Nd}_{0.4}\text{Sr}_{0.12}\text{CuO}_4$ . The Bose factor has been divided out, a fitted background (linear in  $h$ ) has been subtracted, and a correction has been made for differences in resolution volume at the two energies. Panels on the left correspond to  $\hbar\omega = 2$  meV and temperatures of (a) 72 K, (b) 68 K, (c) 50 K; on the right,  $\hbar\omega = 3$  meV and temperatures are (d) 72 K, (e) 68 K, (f) 50 K. Measured at H4M using a fixed incident energy of 14.7 meV, horizontal collimations =  $40'-120'-80'-80'$ , and typical counting time of 20 min per point. Solid lines are Gaussians fit with the constraint that the peaks be symmetric about  $h = 0.5$ .

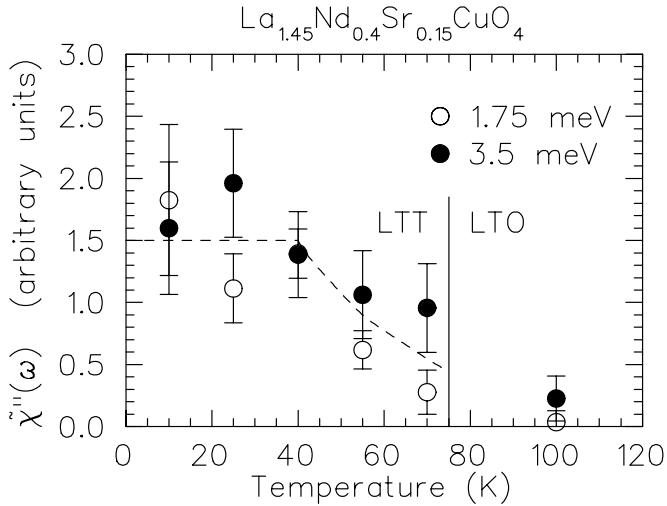


FIG. 7.  $Q$ -integrated  $\chi''(Q, \omega)$  for  $\text{La}_{1.45}\text{Nd}_{0.4}\text{Sr}_{0.15}\text{CuO}_4$  obtained from scans similar to those in the previous figure. The vertical line indicates the LTT-LTO phase boundary, and the dashed line is a guide to the eye.

curve in (a) is a fit based on a disordered stripe model described in Ref. 45. The peak in (b), which is resolution limited, is clearly much narrower than that in (a). Such a difference appears to be consistent with the more dynamic nature of the correlations in the  $x = 0.15$  sample with no Nd.

The inelastic  $Q$  width at 2 meV in  $\text{La}_{2-x}\text{Sr}_x\text{CuO}_4$  with  $x = 0.12$  has recently been reported by Yamada *et al.*<sup>10</sup> They find a value essentially the same as the resolution-limited width that we observe at 3 meV in the Nd-doped crystal. An elastic magnetic signal at the same incommensurate position has also been discovered in the  $x = 0.12$  crystal with no Nd.<sup>12</sup> Thus, there seems to be a reasonable correlation between decreasing inelastic  $Q$ -widths (perhaps limited by the correlation length) and the onset of static order.

Before moving on, we should consider whether the effective spin-wave velocity discussed in the last section is consistent with the observed peak width (half-width =  $0.012 \text{ \AA}^{-1}$ ) in Fig. 8(b). If the width were determined entirely by dispersion, rather than resolution, then the corresponding spin-wave velocity is  $\sim 250 \text{ meV}\cdot\text{\AA}$ . This is almost 3 times greater than the estimate we obtained for  $\hbar c_{\text{eff}}$  from  $\kappa(T)$ . Part of the discrepancy might be associated with anisotropy in the dispersion; however, attempts to test this experimentally have so far been limited by anisotropy in the resolution function. Clearly, more work is required to obtain a consistent quantitative account of the quasi-elastic and inelastic scattering.

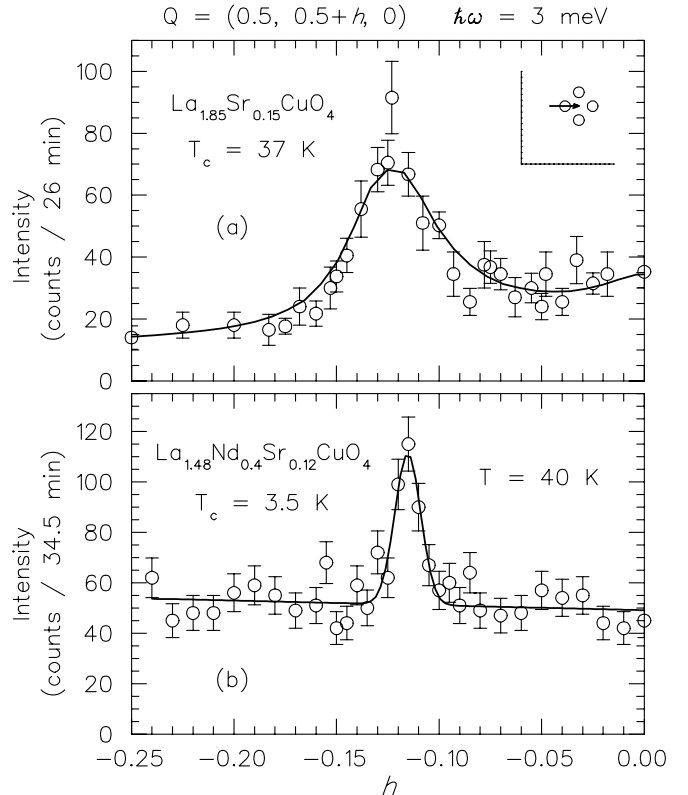


FIG. 8. Comparison of constant-energy scans at  $\hbar\omega = 3 \text{ meV}$  through an incommensurate magnetic peak (see inset) for (a)  $\text{La}_{1.85}\text{Sr}_{0.15}\text{CuO}_4$  (Ref. 46, 47), and (b)  $\text{La}_{1.48}\text{Nd}_{0.4}\text{Sr}_{0.12}\text{CuO}_4$  (crystal U2). Both measurements were performed with a fixed incident energy of 14.7 meV and a sample temperature of 40 K. Scan (a) was done at H7 with horizontal collimations of  $40'-40'-40'-80'$ , while (b) was done at H4M with  $40'-80'-80'-80'$ . Fitted curves are discussed in the text.



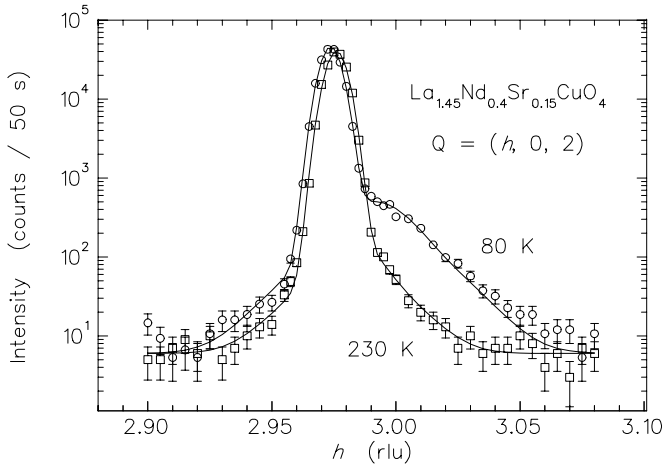


FIG. 9. Elastic scans along  $Q = (h, 0, 2)$  at two different temperatures for  $\text{La}_{1.45}\text{Nd}_{0.4}\text{Sr}_{0.15}\text{CuO}_4$ . Note that the intensity is plotted on a logarithmic scale. The strong peak at  $h \approx 2.975$  corresponds to the LTO-allowed  $(032)_o$  superlattice peak. The broad feature centered near  $h = 3$  at 80 K is diffuse scattering associated with the  $(302)$  reflection, which is forbidden in LTO but allowed in LTT and LTLO. The fitted curves are discussed in the text.

## VI. IMPERFECT STRUCTURAL ORDER IN THE LTO PHASE

We now return our attention to the structural order of the  $x = 0.15$  crystal in the LTO phase. In section III we noted the presence of a broad, unexpected peak between the  $(040)_o$  and  $(400)_o$  Bragg reflections [see Fig. 3(a)]. The position of the broad peak suggests a tetragonal (or less-orthorhombic) component, and the width corresponds to domains of width  $\sim 140$  Å. To test whether this component is consistent with LTT-like domains, we looked for related scattering near a characteristic superlattice position. Figure 9 shows scans along  $\mathbf{Q} = (h, 0, 2)_o$  (note the logarithmic intensity scale). The strong peak at  $h \approx 2.975$  is the allowed  $(032)_o$  of the LTO phase; the noninteger value of  $h$  is due to the slight orthorhombic splitting between  $a^*$  and  $b^*$ . In the 80 K scan, one can see a second peak, broad and weak, that is centered at  $h \approx 3.00$ . Such a peak is not allowed in the LTO phase, but would be expected in the LTT. Its intensity has diminished considerably in the scan at 230 K.

To analyze the temperature dependence of the diffuse  $(302)_o$  scattering, we restricted our choice of fitting functions to Gaussians. (Lorentzians were rejected because of the significant peak area associated with tails outside of the measurement region.) A single gaussian was used for the  $(032)_o$  peak, but was found to give a poor fit to  $(302)_o$ . A more satisfactory fit was obtained using the following combination of two Gaussians:

$$I(h) = A \left[ e^{-\frac{1}{2}(h-h_0)^2/\sigma^2} + \frac{1}{2}e^{-\frac{1}{2}(h-h_0)^2/(2\sigma)^2} \right]. \quad (6)$$

Typical fits are indicated by the curves through the data

points in Fig. 9. At 80 K, the peak center,  $h_0$ , is 2.992(2), and the widths of the two Gaussian peaks correspond to domain sizes of 180 Å and 90 Å. The average of these lengths is similar to the value obtained from the broad  $(400)_o$  peak. As the peak width does not vary significantly with temperature, the intensity reflects the volume fraction of LTT-like domains within the LTO matrix.

The temperature dependence of the  $(302)_o$  intensity is plotted in Fig. 10(a). The intensity varies little at high temperature, but it begins to grow rapidly at lower temperatures. As indicated by the curve through the data points, the temperature dependence is described well by a function of the form  $a + b/T^3$ . The significance of the temperature independent term is not clear. As one can see in the 230-K scan in Fig. 9, the diffuse peak becomes difficult to distinguish from possible (very weak) tails on the strong  $(032)_o$  peak. Thus, it is possible that the scattering from LTT-like domains actually disappears at room temperature.

It is interesting to compare the temperature dependence of the  $(302)_o$  scattering with that of the in-plane resistivity. In the LTO phase,  $\rho_{ab}$  is nearly linear in temperature, just as is observed for samples with no Nd; however, a slight deviation from linearity begins to become noticeable below 150 K. To examine this deviation, we first fit the data between 170 and 300 K to the form

$$\rho_{ab} = \rho_0 + \rho_T T, \quad (7)$$

finding  $\rho_0 = -0.01 \mu\Omega\text{-cm}$  and  $\rho_T = 1.26 \times 10^{-3} \mu\Omega\text{-cm/K}$ . Extrapolating the linear contribution and subtracting from the data gives  $\Delta\rho_{ab}$ , which is plotted in Fig. 10(b). As one can see,  $\Delta\rho_{ab}$  grows at low temperature in a fashion similar to the  $(302)_o$  intensity. In fact, the temperature dependence is well described by the same functional form, as indicated by the curve through the data points.

Given the evident correlation between the  $(302)_o$  intensity and  $\Delta\rho_{ab}$ , we speculate that the rise in  $\Delta\rho_{ab}$  is associated with charge-stripe pinning in the LTT-like domains which occupy a small volume fraction of the sample. Electron-diffraction studies of  $\text{La}_{1.88}\text{Ba}_{0.12}\text{CuO}_4$  and  $\text{La}_{1.5}\text{Nd}_{0.4}\text{Sr}_{0.1}\text{CuO}_4$  indicate that LTT-like domains first appear at the LTO twin boundaries.<sup>48,49,50</sup> If LTT-like domains uniformly decorate all LTO twin boundaries, then it may be difficult for an electron (or hole) to move through the sample without passing through a region of pinned or nearly-pinned charge stripes. The continuous development of the LTT-like volume fraction and its impact on the resistivity may explain, at least in part, why the resistivity does not clearly reflect the temperature dependence of the charge order parameter determined by diffraction.<sup>7,23</sup>

## VII. SUMMARY AND DISCUSSION

We have presented neutron scattering studies of various aspects of ordering in crystals of

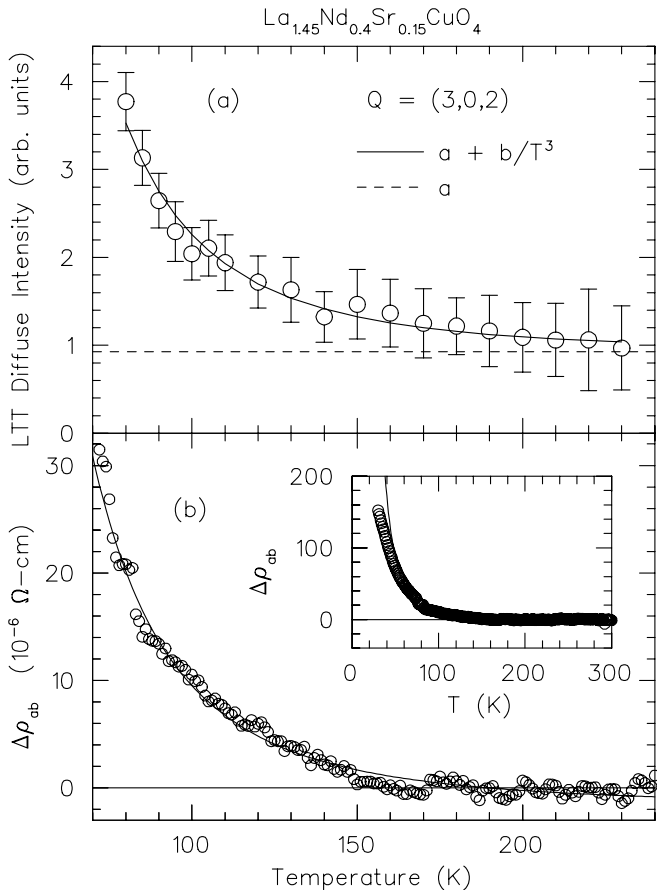


FIG. 10. (a) Temperature dependence of the diffuse intensity centered at  $Q = (3, 0, 2)$ , for  $\text{La}_{1.45}\text{Nd}_{0.4}\text{Sr}_{0.15}\text{CuO}_4$ . Solid line is a fit to the form  $I = a + b/T^3$ ; dashed line indicates the temperature-independent term. (b) In-plane resistivity remaining after subtraction of a dominant contribution linear in  $T$ , determined from a fit over the range  $170 \text{ K} \leq T \leq 300 \text{ K}$ . The line through the data is a fit to the form  $\Delta\rho_{ab} = a + b/T^3$ . The inset shows the data and fit over a larger temperature range.

$\text{La}_{1.6-x}\text{Nd}_{0.4}\text{Sr}_x\text{CuO}_4$  with  $x = 0.12$  and  $0.15$ . The most significant results are the following: 1) At low temperature, where the Cu spins order in a nearly two-dimensional stripe structure, the magnetic correlation length remains finite. 2) The temperature dependence of the correlation length above 30 K is similar to that of the renormalized-classical regime of a 2D Heisenberg antiferromagnet, and applying the formula for the spin-only system yields a measure of the effect that the charge stripes have on the effective spin-wave velocities. 3) Within the LTO phase, there is a correlation between the deviation of the resistivity from a linear temperature dependence and the volume fraction of LTT-like domains. Below, each of these points will be discussed in turn.

### A. Finite correlation length

What can we say about the nature of the magnetic disorder in the ground state of the  $x = 0.12$  sample? One possible model would be isolated, ordered domains of finite size within a sea of disorder; however, such a picture is in conflict with the zero-field  $\mu\text{SR}$  observation that essentially every muon implanted in such a sample sees a local hyperfine field.<sup>22</sup> There appear to be no significant regions of the sample that do not show local magnetic order. An alternative model that allows local order everywhere involves disorder in the spacing between charge stripes. One assumes that the charge stripes are separated by an integral number of lattice spacings, and that at least two distinct stripe periods exist. Such a model is consistent with the idea that commensurability with the lattice should play a role in the pinning of stripes in the LTT phase. Furthermore, as we will see, it is compatible with the incommensurate peak splitting,<sup>7</sup>  $\epsilon = 0.118$ .

Formulas for calculating the scattered intensity from a random mixture of 2 structural units were first worked out by Hendricks and Teller.<sup>51,52</sup> (One of us used these formulas previously<sup>53</sup> to model staging disorder associated with interstitial oxygens in  $\text{La}_2\text{NiO}_{4+\delta}$ .) As structural units we take magnetic unit cells of period  $8a$  and  $10a$ . (Each of these corresponds to two unit cells of the corresponding charge modulation.) Within each unit, we consider only Cu sites, and assume, for simplicity, a sinusoidal variation of the spin density. The atomic displacements associated with the charge modulation are also taken to be sinusoidal.

Within the model, the only free parameter is the ratio of the occurrence probabilities for the two structural units. We adjusted this value to make the peaks associated with spin modulation appear at positions consistent with experiment. This criterion was satisfied with a probability of 75% for the  $8a$  unit and 25% for the  $10a$  unit. The resulting scattered intensities due to the spin and lattice modulations are shown in Fig. 11 as a function of momentum (in reciprocal lattice units) along the modulation direction. To extract peak positions and widths

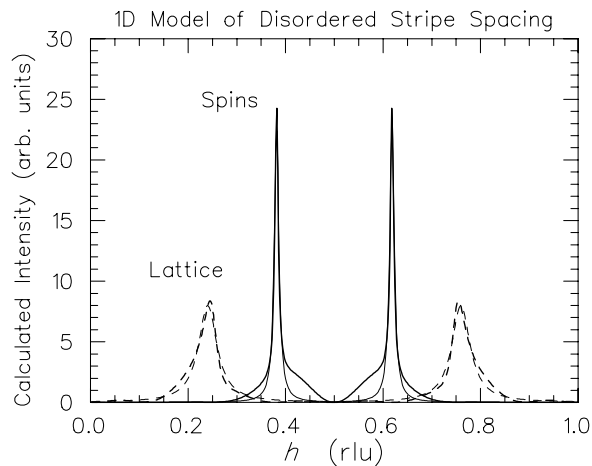


FIG. 11. Calculated scattered intensity as a function of  $h$  for the model of 1D stripe-spacing disorder discussed in the text. Thick solid line: scattering due to spins; thick dashed line: signal due to lattice modulation. Thin lines represent fitted Lorentzians.

TABLE I. Values for effective  $\epsilon$  (from peak position) and half-width at half maximum (HWHM) obtained from Lorentzian fits to the disordered-stripe model calculation shown in Fig. 11.

Peak	$\epsilon_{\text{eff}}$ (rlu)	HWHM ( $10^{-3} \text{ \AA}^{-1}$ )
Spin	0.118	9.5
Lattice	0.120	38.3

for comparison with experiment, Lorentzians were fit to the calculated intensity. The results are listed in Table I.

It is obvious from the figure and the fitted values in the table that the disorder assumed in the model yields finite peak widths that are larger for the lattice peaks than for the spin peaks. The width for magnetic peaks in this simple model is about twice what we have found experimentally, and the same discrepancy is found for the charge order peaks.<sup>23</sup> However, the ratio of calculated widths for lattice peaks relative to spin peaks ( $= 4$ ) is exactly the same as the ratio of the experimentally determined widths.<sup>23</sup> The difference in widths for lattice and spin peaks is easily understood: the scattering from the two distinct unit cells of the model is more nearly in phase at the magnetic wave vector than at the charge-order wave vector. While one could tune the choice of unit cells in the model to obtain better quantitative agreement with experiment, the salient point here is that the experimentally observed peak widths and positions are qualitatively consistent with disorder in the stripe spacing.

What causes the stripe disorder? One possibility is the local potential variations due to the randomly positioned divalent Sr ions. On the other hand, evidence has recently been presented<sup>54</sup> that all variations in cation radius on the La site contribute to the suppression of  $T_c$ , so perhaps the substituted Nd, which is significantly smaller

than the La, makes a contribution to disorder comparable to that of the Sr. The relevance of disorder to pinning charge stripes and the development of glassy order is discussed in Refs. 55, 56.

In applying the Hendricks-Teller model, we have considered disorder in only one direction, perpendicular to the stripes. If the disorder is induced by randomly positioned Sr and Nd substituents, then there should also be defects, such as dislocations, along the stripes. Equal probabilities for defects in parallel and perpendicular directions would explain the absence of a detectable anisotropy in scattering peak width.

## B. Temperature-dependence of the correlation length

We have seen that the magnetic peak width begins to grow for temperatures above 30 K, the point at which  $\mu\text{SR}$  measurements<sup>22</sup> indicate the disappearance of static magnetic order. Given the finite widths for both the magnetic and charge-order peaks at low temperature, it is reasonable to ask whether the decrease in the magnetic correlation might be due to increasing disorder (perhaps dynamic) in the positions of the charge stripes. According to the Hendricks-Teller model applied above, such an increase in charge stripe disorder should be reflected in a relative growth in the charge-order peak width comparable to that of the magnetic peaks. However, the charge-order width observed in the X-ray diffraction measurements<sup>23</sup> shows little variation up to 65 K. Hence, it appears most likely that the charge stripe configuration remains static throughout the region in which the magnetic width is observed to vary.

It seems reasonable, then, to analyze the decrease of the magnetic correlation length in terms of spin fluctuations within well defined domains. In section IV we considered the implications of an effective anisotropic Heisenberg model first proposed by Castro Neto and Hone.<sup>24,25</sup> The temperature dependence of  $\kappa$  is well described by the renormalized-classical behavior predicted by the analysis of the model; however, the effective spin-wave velocity perpendicular to the stripes implied by the fit to the model appears to be inconsistent with the measurements of the spin fluctuations at  $\hbar\omega = 3 \text{ meV}$ . The model can be improved by considering the enhanced quantum effects that occur when the magnetic domains correspond to even-legged spin ladders. The latter model appears to run into trouble when one tries to consider the doping dependence of the magnetic correlations, since magnetic order is most robust<sup>11,43,14</sup> at  $x \approx \frac{1}{8}$ .

It is quite possible that the interaction between the holes in the domain walls and the spins in the domains is not adequately characterized in terms of an effective exchange coupling between antiferromagnetic domains. An alternative model of the interaction has been evaluated by Emery, Kivelson, and Zachar.<sup>8</sup> They find that the interaction takes place by the hopping of pairs of holes from

a charge stripe into the magnetic regions, and that the pair hopping tends to enhance singlet correlations. This picture would certainly be consistent with a weak effective coupling between neighboring domains; however, a specific prediction for the low-energy spin fluctuations relevant to the present case has not been made.

### C. Correlation between resistivity and structure

For crystals of  $\text{La}_{1.6-x}\text{Nd}_{0.4}\text{Sr}_x\text{CuO}_4$  with  $x$  near  $\frac{1}{8}$ , the in-plane resistivity shows<sup>57</sup> an abrupt upward jump on transforming to the LTT structure near 70 K. When Nd is replaced by Eu, the LTT transition shifts up to approximately 130 K, and no jump in resistivity is found.<sup>58</sup> Instead, on cooling there is a continuous deviation from a linear temperature dependence, with a significant upturn below 50 to 60 K. In light of that, the correlation between resistivity and LTT-like volume fraction above 80 K in our Nd-doped  $x = 0.15$  sample should perhaps come as no surprise.

It seems reasonable to assume that the rise in resistivity on cooling is associated with pinning of the charge stripes. If the charge order were like that in a conventional CDW system, in which a gap opens over a significant portion of the Fermi surface, then one might expect to see the charge order parameter directly reflected in the resistivity. So far, infrared reflectivity studies have provided no evidence for a charge gap,<sup>19</sup> and such a gap would appear to be incompatible with the superconductivity observed in the  $x = 0.15$  sample.<sup>11,20,21,22</sup> On the other hand, the gradual increase in resistivity is consistent with the glass-like stripe disorder that was analyzed above. Also, a recent study of the CDW system  $\text{TaS}_2$  has shown that a very small amount of disorder in that system can suppress the transition to commensurate CDW order and the concomitant jump in resistivity.<sup>59</sup> It has been argued recently that transverse fluctuations of charge stripes are important for suppressing CDW order along the stripes.<sup>32</sup> Perhaps static disorder caused by randomly positioned dopants can also frustrate true CDW order.

### ACKNOWLEDGMENTS

We are pleased to acknowledge stimulating discussions with R. J. Birgeneau, A. H. Castro Neto, D. Hone, A. R. Moodenbaugh, G. Shirane, J. Zaanen, and especially with V. J. Emery and S. A. Kivelson. Assistance from J. D. Axe in the early stages of this work is greatly appreciated. This research has received some support from the U.S.-Japan Cooperative Neutron-Scattering Program. Work at Brookhaven was carried out under Contract No. DE-AC02-98CH10886, Division of Materials Sciences, U.S. Department of Energy.

- 
- <sup>1</sup> A. R. Moodenbaugh, Y. Xu, M. Suenaga, T. J. Folkerts, and R. N. Shelton, *Phys. Rev. B* **38**, 4596 (1988).
  - <sup>2</sup> J. D. Axe, A. H. Moudden, D. Hohlwein, D. E. Cox, K. M. Mohanty, A. R. Moodenbaugh, and Y. Xu, *Phys. Rev. Lett.* **62**, 2751 (1989).
  - <sup>3</sup> T. Suzuki and T. Fujita, *Physica C* **159**, 111 (1989).
  - <sup>4</sup> M. K. Crawford, R. L. Harlow, E. M. McCarron, W. E. Farneth, J. D. Axe, H. Chou, and Q. Huang, *Phys. Rev. B* **44**, 7749 (1991).
  - <sup>5</sup> B. Büchner, M. Breuer, A. Freimuth, and A. P. Kampf, *Phys. Rev. Lett.* **73**, 1841 (1994).
  - <sup>6</sup> J. M. Tranquada, B. J. Sternlieb, J. D. Axe, Y. Nakamura, and S. Uchida, *Nature* **375**, 561 (1995).
  - <sup>7</sup> J. M. Tranquada, J. D. Axe, N. Ichikawa, Y. Nakamura, S. Uchida, and B. Nachumi, *Phys. Rev. B* **54**, 7489 (1996).
  - <sup>8</sup> V. J. Emery, S. A. Kivelson, and O. Zachar, *Phys. Rev. B* **56**, 6120 (1997).
  - <sup>9</sup> S.-W. Cheong, G. Aeppli, T. E. Mason, H. Mook, S. M. Hayden, P. C. Canfield, Z. Fisk, K. N. Clausen, and J. L. Martinez, *Phys. Rev. Lett.* **67**, 1791 (1991).
  - <sup>10</sup> K. Yamamoto, T. Katsufuji, T. Tanabe, and Y. Tokura, *Phys. Rev. Lett.* **80**, 1493 (1998).
  - <sup>11</sup> J. M. Tranquada, J. D. Axe, N. Ichikawa, A. R. Moodenbaugh, Y. Nakamura, and S. Uchida, *Phys. Rev. Lett.* **78**, 338 (1997).
  - <sup>12</sup> T. Suzuki, T. Goto, K. Chiba, T. Shinoda, T. Fukase, H. Kimura, K. Yamada, M. Ohashi, and Y. Yamaguchi, *Phys. Rev. B* **57**, R3229 (1998).
  - <sup>13</sup> K. Hirota, K. Yamada, I. Tanaka, and H. Kojima, *Physica B* **241-243**, 817 (1998).
  - <sup>14</sup> H. Kimura, K. Hirota, H. Matsushita, K. Yamada, Y. E. S.-H. Lee, C. F. Majkrzak, R. Erwin, G. Shirane, M. Greven, Y. S. Lee, M. A. Kastner, and R. J. Birgeneau, (preprint).
  - <sup>15</sup> Y. S. Lee, R. J. Birgeneau, M. A. Kastner, Y. Endoh, S. Wakimoto, K. Yamada, R. W. Erwin, S.-H. Lee, and G. Shirane, *cond-mat/9902157*.
  - <sup>16</sup> P. Dai, H. A. Mook, and F. Doğan, *Phys. Rev. Lett.* **80**, 1738 (1998).
  - <sup>17</sup> H. A. Mook, P. Dai, S. M. Hayden, G. Aeppli, T. G. Perring, and F. D. gan, *Nature* **395**, 580 (1998).
  - <sup>18</sup> G. Grüner, *Rev. Mod. Phys.* **60**, 1129 (1988).
  - <sup>19</sup> S. Tajima, N. L. Wang, M. Takaba, N. Ichikawa, and S. Uchida, *J. Phys. Chem. Solids* **59**, 2015 (1998).
  - <sup>20</sup> J. E. Ostenson, S. Bud'ko, M. Breitwisch, D. K. Finnemore, N. Ichikawa, and S. Uchida, *Phys. Rev. B* **56**, 2820 (1997).
  - <sup>21</sup> A. R. Moodenbaugh, L. H. Lewis, and S. Soman, *Physica C* **290**, 98 (1997).
  - <sup>22</sup> B. Nachumi, Y. Fudamoto, A. Keren, K. M. Kojima, M. Larkin, G. M. Luke, J. Merrin, O. Tchernyshyov, Y. J. Uemura, N. Ichikawa, M. Goto, S. Uchida, M. K. Crawford, E. M. McCarron, D. E. MacLaughlin, and R. H. Heffner, *Phys. Rev. B* **58**, 8760 (1998).
  - <sup>23</sup> M. v. Zimmermann, A. Vigliante, T. Niemöller, N. Ichikawa, T. Frello, S. Uchida, N. H. Andersen, J. Madsen, P. Wochner, J. M. Tranquada, D. Gibbs, and J. R.

- Schneider, *Europhys. Lett.* **41**, 629 (1998).
- <sup>24</sup> A. H. Castro Neto and D. Hone, *Phys. Rev. Lett.* **76**, 2165 (1996).
- <sup>25</sup> C. N. A. van Duin and J. Zaanen, *Phys. Rev. Lett.* **80**, 1513 (1998).
- <sup>26</sup> J. Tworzydło, O. Y. Osman, C. N. A. van Duin, and J. Zaanen, *Phys. Rev. B* **59**, 115 (1999).
- <sup>27</sup> Y. J. Kim, R. J. Birgeneau, M. A. Kastner, Y. S. Lee, Y. Endoh, G. Shirane, and K. Yamada, (preprint).
- <sup>28</sup> J. D. Axe and M. K. Crawford, *J. Low Temp. Phys.* **95**, 271 (1994).
- <sup>29</sup> A. R. Moodenbaugh, L. Wu, Y. Zhu, L. H. Lewis, and D. E. Cox, *Phys. Rev. B* **58**, 9549 (1998).
- <sup>30</sup> S. Shamoto, T. Kiyokura, M. Sato, K. Kakurai, Y. Nakamura, and S. Uchida, *Physica C* **203**, 7 (1992).
- <sup>31</sup> B. Büchner, M. Cramm, M. Braden, W. Braunisch, O. Hofels, W. Schnelle, R. Müller, A. Freimuth, W. Schlabitz, G. Heger, D. I. Khomskii, and D. Wohlleben, *Europhys. Lett.* **21**, 953 (1993).
- <sup>32</sup> S. A. Kivelson, E. Fradkin, and V. J. Emery, *Nature* **393**, 550 (1998).
- <sup>33</sup> P. M. Chaikin and T. C. Lubensky, *Principles of condensed matter physics* (Cambridge University Press, Cambridge, UK, 1995).
- <sup>34</sup> B. J. Sternlieb, G. M. Luke, Y. J. Uemura, T. M. Riseman, J. H. Brewer, P. M. Gehring, K. Yamada, Y. Hidaka, T. Murakami, T. R. Thurston, and R. J. Birgeneau, *Phys. Rev. B* **41**, 8866 (1990).
- <sup>35</sup> B. Keimer, N. Belk, R. J. Birgeneau, A. Cassanho, C. Y. Chen, M. Greven, M. A. Kastner, A. Aharony, Y. Endoh, R. W. Erwin, and G. Shirane, *Phys. Rev. B* **46**, 14034 (1992).
- <sup>36</sup> S. Chakravarty, B. I. Halperin, and D. R. Nelson, *Phys. Rev. Lett.* **60**, 1057 (1988).
- <sup>37</sup> S. Chakravarty, B. I. Halperin, and D. R. Nelson, *Phys. Rev. B* **39**, 2344 (1989).
- <sup>38</sup> S. M. Hayden, G. Aeppli, R. Osborn, A. D. Taylor, T. G. Perring, S.-W. Cheong, and Z. Fisk, *Phys. Rev. Lett.* **67**, 3622 (1991).
- <sup>39</sup> G. Aeppli, S. M. Hayden, H. A. Mook, A. Fisk, S.-W. Cheong, D. Rytz, J. P. Remeika, G. P. Espinosa, and A. S. Cooper, *Phys. Rev. Lett.* **62**, 2052 (1989).
- <sup>40</sup> M. Matsuda, K. Yamada, Y. Endoh, T. R. Thurston, G. Shirane, R. J. Birgeneau, M. A. Kastner, I. Tanaka, and H. Kojima, *Phys. Rev. B* **49**, 6958 (1994).
- <sup>41</sup> G. Aeppli, T. E. Mason, S. M. Hayden, H. A. Mook, and J. Kulda, *Science* **278**, 1432 (1997).
- <sup>42</sup> S. R. White and D. J. Scalapino, *Phys. Rev. Lett.* **80**, 1272 (1998).
- <sup>43</sup> K. Kumagai, K. Kawano, I. Watanabe, K. Nishiyama, and K. Nagamine, *Hyperfine Int.* **86**, 473 (1994).
- <sup>44</sup> K. Yamada, K. Kakurai, Y. Endoh, T. R. Thurston, M. A. Kastner, R. J. Birgeneau, G. Shirane, Y. Hidaka, and T. Murakami, *Phys. Rev. B* **40**, 4557 (1989).
- <sup>45</sup> J. M. Tranquada, *Physica C* **282–287**, 166 (1997).
- <sup>46</sup> B. J. Sternlieb and G. Shirane, (unpublished).
- <sup>47</sup> K. Yamada, S. Wakimoto, G. Shirane, C. H. Lee, M. A. Kastner, S. Hosoya, M. Greven, Y. Endoh, and R. J. Birgeneau, *Phys. Rev. Lett.* **75**, 1626 (1995).
- <sup>48</sup> C. H. Chen, S.-W. Cheong, and A. S. Cooper, *Phys. Rev. Lett.* **71**, 2461 (1993).
- <sup>49</sup> Y. Zhu, A. R. Moodenbaugh, Z. X. Cai, J. Taftø, M. Suenaga, and D. O. Welch, *Phys. Rev. Lett.* **73**, 3026 (1994).
- <sup>50</sup> Y. Inoue, Y. Horibe, and Y. Koyama, *Phys. Rev. B* **56**, 14176 (1997).
- <sup>51</sup> S. Hendricks and E. Teller, *J. Chem. Phys.* **10**, 147 (1942).
- <sup>52</sup> J. Kakinoki and Y. Komura, *J. Phys. Soc. Jpn.* **7**, 30 (1952).
- <sup>53</sup> J. M. Tranquada, Y. Kong, J. E. Lorenzo, D. J. Buttrey, D. E. Rice, and V. Sachan, *Phys. Rev. B* **50**, 6340 (1994).
- <sup>54</sup> J. P. Attfield, A. L. Kharlanov, and J. A. McAllister, *Nature* **394**, 157 (1998).
- <sup>55</sup> S. A. Kivelson and V. J. Emery, cond-mat/9809083.
- <sup>56</sup> N. Hasselmann, A. H. Castro Neto, C. Morais Smith, and Y. Dimashko, cond-mat/9807070.
- <sup>57</sup> Y. Nakamura and S. Uchida, *Phys. Rev. B* **46**, 5841 (1992).
- <sup>58</sup> M. Hücker, V. Kataev, J. Pommer, O. Baberski, W. Schlabitz, and B. Büchner, *J. Phys. Chem. Solids* **59**, 1821 (1998).
- <sup>59</sup> F. Zwick, H. Berger, I. Vobornik, G. Margaritondo, L. Forró, C. Beeli, M. Onellion, G. Panaccione, A. Taleb-Ibrahimi, and M. Grioni, *Phys. Rev. Lett.* **81**, 1058 (1998).